

Plasmon Modes and Correlation Functions in Quantum Wires and Hall Bars

U. Zülicke and A. H. MacDonald

Department of Physics, Indiana University, Bloomington, Indiana 47405, U.S.A.

(October 9, 2018)

We present microscopic derivations of the one-dimensional low-energy boson effective Hamiltonians of quantum wire and quantum Hall bar systems. The quantum Hall system is distinguished by its spatial separation of oppositely directed electrons. We discuss qualitative differences in the plasmon collective mode dispersions and the ground state correlation functions of the two systems which are consequences of this difference. The slowly-decaying quasi-solid correlations expected in a quantum wire are strongly suppressed in quantum Hall bar systems.

PACS numbers: 73.20.Mf, 73.40.Hm, 72.15.Nj, 71.10.Pm

I. INTRODUCTION

The quantum Hall effect occurs in two-dimensional (2D) electron systems (ES) when the chemical potential lies in a charge gap which occurs at a density (n^*) which is dependent on magnetic field (B). The B dependence of n^* requires¹ gapless excitations localized at the edge of the 2D ES. The low-energy effective Hamiltonian which describes this edge system is simplest when the edge is sharp² on a microscopic length scale and the bulk Landau level filling factor $\nu^* = 2\pi\ell^2 n^* = 1/m$ with m being an odd integer. In this case, the low-energy edge excitations can be mapped to those of a one-dimensional (1D) fermion system^{3,4} and described^{5,6} by a version of the Tomonaga-Luttinger (TL) model for 1D fermion systems⁷⁻⁹ modified to account for the magnetic field and the long-range of the electron-electron interaction. Edge excitations in quantum Hall (QH) bars are analogous to the excitations of electron systems in quantum wires¹⁰ which are also described at low energies by a TL model modified to account for long-range interactions. Close relationships exist between studies of the effect of Coulomb interactions on the transport properties of QH systems^{11,12} and analogous studies of quantum wires.^{13,14} There are, however, important distinctions between these two systems which result from the spatial separation of oppositely directed electrons in the QH case and are the subject of this paper. As we explain below, the energy-wavevector relationship for the plasmon boson states of quantum wires and QH bars have quite different microscopic underpinnings. In addition, the strong quasi-solid correlations expected¹⁵ in a quantum wire are suppressed in typical Hall bar systems.¹⁶

II. NON-INTERACTING ELECTRONS

The analogy between quantum wires and quantum Hall bars is most direct for $\nu = 1$ and we begin by discussing this case, first for non-interacting electrons. To form a quantum wire, electrons in a 2D ES are confined in an additional direction, say the \hat{y} -direction, while the motion in the remaining (\hat{x} -)direction stays free. With periodic boundary conditions applied over a length L in the \hat{x} -direction, the electronic single-particle wave functions then have the form

$$\psi_{n,k}^{\text{QW}}(x, y) = \frac{1}{\sqrt{L}} e^{ikx} \chi_n^{\text{QW}}(y) \quad (1)$$

where $\chi_n^{\text{QW}}(y)$ is the n -th discrete subband state for the quantum wire. The single-particle eigenenergy $\varepsilon_{n,k} = E_n + \hbar^2 k^2 / 2m^*$. For wires widths comparable to or smaller than the typical distance between electrons, the energy spacing between different subbands will be larger than the Fermi energy and only the lowest ($n = 0$) subband will be occupied in the ground and low-energy excited states. The ground state of the non-interacting many-electron system is a 1D Fermi gas state in which all single-particle states with $n = 0$ and $|k| \leq k_F$ are occupied. The subband wavefunction leads only to form factors which will modify the electron-electron interaction in the system at short distances. The situation for a 2D ES in a strong perpendicular magnetic field is similar. For a Hall bar geometry where the system is confined in the \hat{y} -direction and periodic boundary conditions are applied in the \hat{x} -direction, the Landau gauge [$\vec{A} = (-By, 0, 0)$] wavefunctions have the form¹⁷

$$\psi_{n,k}^{\text{HB}}(x, y) = \frac{1}{\sqrt{L}} e^{ikx} \chi_n^{\text{HB}}(y - \ell^2 k) . \quad (2)$$

Here $\ell := [\hbar c / (eB)]^{1/2}$ is the magnetic length, n is the Landau level index, and $\chi_n^{\text{HB}}(y)$ is the wave function of a harmonic oscillator with frequency $\omega_c = eB / (m^* c)$ which is localized to a length $\sim \ell$ around $y = 0$. The oscillator wavefunctions play the role of the subband wavefunction in a quantum wire, but in the Hall bar case they are displaced from the origin by a distance proportional to wave vector k . In addition, the dependence of the single-particle eigenenergy, $\varepsilon_{n,k} = \hbar\omega_c(n + 1/2) + V^{\text{ext}}(\ell^2 k)$, on k is due to the confinement potential $V^{\text{ext}}(y)$ rather than to the kinetic energy. In the strong magnetic field limit, only $n = 0$ states will be occupied at $\nu = 1$, even when the width of the Hall bar is macroscopic, and states at the Fermi energy with $k = \pm k_F$ will be localized at

opposite edges of the sample, as illustrated in Fig. 1. This property of Hall bar systems plays the central role in the edge state picture of the integer quantum Hall effect for non-interacting electrons.^{3,18} The sample width $W = 2k_F\ell^2$ is assumed to be much larger than the magnetic length ℓ throughout this paper. When this condition is not satisfied the distinction between a quantum wire and a quantum Hall bar blurs.

III. COULOMB MATRIX ELEMENTS AND LOW-ENERGY HAMILTONIAN

Quantum wire and QH bar systems are described by microscopic Hamiltonians of the same form

$$H = H^0 + H^{\text{int}} \quad (3a)$$

$$H^0 = \sum_k \hbar(|k| - k_F) v_F c_k^\dagger c_k \quad (3b)$$

$$H^{\text{int}} = \frac{1}{2L} \sum_{k,p,q} V(k,p,q) c_{k+q}^\dagger c_p^\dagger c_{p+q} c_k \quad (3c)$$

where H^0 is the one-body term in the Hamiltonian and the single-particle energy has been linearized around $k = \pm k_F$ so that $v_F = \hbar k_F/m^*$ in the quantum wire case while

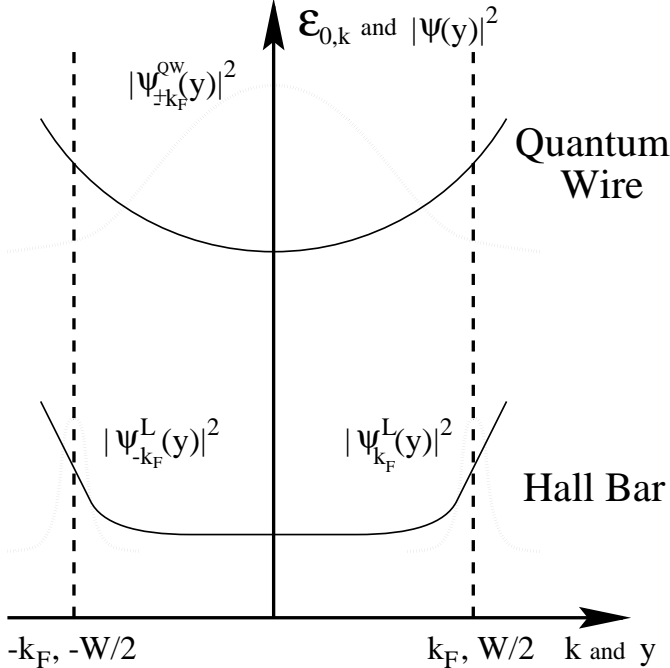


FIG. 1. Comparison of quantum wire and quantum Hall bar systems. Both the dependence of the single-particle energy $\epsilon_{0,k}$ on wave vector k (solid lines) and the spatial extent of the lateral part of the wave function [$\equiv |\psi_{0,k}(y)|^2$ depicted as dotted lines] are shown schematically. The principal difference is the strong localization of $|\psi_{0,\pm k_F}^{\text{HB}}(y)|^2$ at opposite edges of the sample in the Hall bar case, compared to the identity of $|\psi_{0,\pm k_F}^{\text{QW}}(y)|^2$ in the quantum wire case.

$$v_F = \frac{\ell^2}{\hbar} \left. \frac{dV^{\text{ext}}}{dy} \right|_{W/2} \quad (4)$$

in the Hall bar case. The y -dependent part of the wave-functions enters crucially into the form of the matrix element $V(k,p,q)$. For quantum wires,^{19,20} the function $\chi_n^{\text{QW}}(y)$ does not depend on k , and the interaction matrix element is a function of momentum transfer q only. Up to an irrelevant constant, it is then possible to rewrite Eqs. (3) as

$$H_{\text{eff}}^{\text{QW}} = H^0 + \frac{1}{2L} \sum_{q \neq 0} V_q^{\text{QW}} \varrho_q \varrho_{-q} \quad (5)$$

Here $\varrho_q = \sum_k c_{k+q}^\dagger c_k$ is the 1D Fourier transform of the density operator. For Coulomb interaction, the effective 1D potential at small q is^{19,20}

$$V_q^{\text{QW}} = \frac{e^2}{\epsilon} (-2) \ln[\alpha q W] \quad (6)$$

where W is the width of the quantum wire and α is a constant of order unity which depends on the details of the confining potential. In the QH bar, however, single-particle states with different relative momentum are separated in the \hat{y} -direction. (See Fig. 1.) Consequently, the matrix element $V(k,p,q)$ depends on both q and $k-p$. If the originally 2D interaction is $U(\vec{r})$ and has the 2D Fourier transform $U(\vec{q}) = U(q_x, q_y)$, we find that

$$V(k,p,q) = \frac{e^{-\frac{1}{2}(q\ell)^2}}{\ell} \int_{-\infty}^{\infty} d\kappa e^{-\frac{1}{2}\kappa^2} U(q, \kappa\ell^{-1}) e^{i\kappa(k-p)\ell}. \quad (7)$$

For the physically relevant Coulomb interaction in the limit of small momentum transfer $q \leq \ell^{-1}$ we obtain (see also Fig. 2)

$$V(k,p,q) = \frac{e^2}{\epsilon} \begin{cases} 2 \text{K}_0(|q(k-p)\ell^2|) & \text{for } |k-p| > \ell^{-1} \\ -2 \ln[\sqrt{\frac{\gamma}{8}} q\ell] & \text{for } |k-p| \leq \ell^{-1} \end{cases} \quad (8)$$

where ϵ is the host semiconductor dielectric constant, and $\gamma \sim 1.78$ is the exponential of Euler's constant. Corrections to Eq. (8) are analytic in q , in $|k-p|^{-1}$ for large $|k-p|$, and in $|k-p|$ for small $|k-p|$ and are negligible for our purposes. Similar expressions for two-particle Coulomb matrix elements in a Hall bar have been reported previously.²¹⁻²⁴ Here we want to use this expression to derive a 1D effective Hamiltonian similar to Eq. (5), to describe the low-energy excitations of a Hall bar. It is useful to separate the $q = 0$ term in the Hamiltonian which, in contrast to the quantum wire case, is not a constant. Defining $\hat{V}(k-p) := V(k,p,0)$ we find that

$$H^{\text{HB}} = H^0 + H^{q=0} + H^{\text{TL}} \quad (9)$$

where

$$H^{q=0} = \frac{1}{2L} \sum_{k,p} \tilde{V}(k-p) c_k^\dagger c_p^\dagger c_p c_k \quad (10a)$$

$$\simeq \frac{1}{L} \sum_k \left[\sum_{p=-k_F}^{k_F} \tilde{V}(k-p) \right] c_k^\dagger c_k \quad (10b)$$

The last line holds in the low-energy sector of the Hamiltonian where number operator fluctuations are negligible except for single-particle states close to the edge of the system which do not contribute importantly to the sum. $H^{q=0}$ simply adds the electrostatic (Hartree) contribution to the single-particle energies which would be present in a Hartree self-consistent field theory. This contribution is an irrelevant constant for a quantum wire but is state dependent in a Hall bar. The Hartree energy is positive and smaller in magnitude for states with $|k| > k_F$ since they are localized farther from the other electrons. Linearizing the Hartree single-particle energy we find that for low energies and $W \gg \ell$

$$H_{\text{eff}}^{q=0} = \sum_k \left(-\frac{e^2}{\epsilon\pi} \right) (|k| - k_F) \ln \left[\sqrt{2\gamma} \frac{W}{\ell} \right] c_k^\dagger c_k. \quad (11)$$

The low-energy physics of a 1D ES can be captured in an approximation where the Hamiltonian is projected onto sectors where the number of right going fermions ($N_R := \sum_{k>0} \langle c_k^\dagger c_k \rangle$) and the number of left going fermions ($N_L := \sum_{k<0} \langle c_k^\dagger c_k \rangle$) are fixed. As is well known from studies of TL models⁷⁻⁹ for 1D ES, this projection permits one-body terms linearized around the Fermi points to be expressed in terms of density operators $\varrho_q^{\text{R,L}} := \sum_{k>0} c_{k+q}^\dagger c_k$. ($\varrho_q = \varrho_q^{\text{L}} + \varrho_q^{\text{R}}$) Using this procedure, $H_{\text{eff}}^{q=0}$ can be lumped with the $q \neq 0$ interaction terms in the Hamiltonian to obtain

$$H_{\text{eff}}^{\text{HB}} = H^0 + \frac{1}{L} \sum_{q>0} \{ V_q^{\text{intra}} [\varrho_q^{\text{L}} \varrho_{-q}^{\text{L}} + \varrho_q^{\text{R}} \varrho_{-q}^{\text{R}}] + V_q^{\text{inter}} [\varrho_q^{\text{L}} \varrho_{-q}^{\text{R}} + \varrho_q^{\text{R}} \varrho_{-q}^{\text{L}}] \} \quad (12)$$

where the effective 1D intra-edge and inter-edge interactions are

$$V_q^{\text{intra}} := \frac{e^2}{\epsilon} (-2) \ln \left[\frac{\gamma}{2} q W \right] \text{ and } V_q^{\text{inter}} := \frac{e^2}{\epsilon} 2K_0(qW).$$

Microscopically, the $q \neq 0$ terms in the interaction Hamiltonian represent the loss of exchange energy when a density wave is created in the system. To obtain this result we have used the fact that the dependence of $V(k, p, q)$ on k and p is negligible at small q when k and p are near the same Fermi point and appealed to linearization in setting $|k - p| = W/\ell^2$ when k and p are near opposite Fermi points.

Previous studies addressing the effect of Coulomb interaction in QH systems have used a Hamiltonian of the

form shown in Eq. (12) as starting point. In this work the Hamiltonian implicitly or explicitly contains two undetermined parameters: the bare Fermi velocity v_F appearing in H_0 and a cut-off length, generally assumed to be microscopic, appearing in the expression for V_q^{intra} . In our microscopic analysis, the length appearing in V_q^{intra} is the macroscopic sample width W and v_F , defined by Eq. (4), is dependent on the external potential. However, it is important to realize that the projection onto fixed N_R and N_L sectors obviates the distinction we have made between one-body and two-body terms in the underlying microscopic Hamiltonian. The identification of a bare Fermi velocity associated with the one-body term plays *no role* in the physics. In our analysis, the intra-edge interaction represents the sum of terms originating from the one-body Hartree energy which leads to an attractive effective interaction and the $q \neq 0$ terms in the intra-edge interaction which are repulsive. We could as well have grouped the Hartree term with the one-body term in the Hamiltonian. With this choice, the one-body term would vanish if the external potential originated from a positively-charged background which precisely cancelled the ground state electron charge density. In typical experimental situations the external potential which attracts electrons to the Hall bar is weaker near the edge than in the neutralizing background model frequently used in theoretical model calculations so that the Fermi velocity is negative when the Hartree term is grouped with the one-body terms. The negative Fermi velocity needn't have any physical consequences, however, since in the case of interest the $q \neq 0$ terms in the Hamiltonian stabilize all excitations.

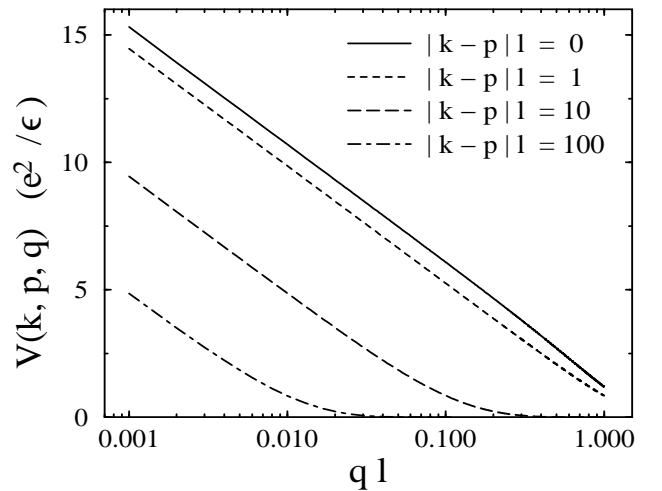


FIG. 2. Matrix element Eq. (7) evaluated for Coulomb interaction. Three regimes can be distinguished if $q\ell < 1$. For the case $|k - p|\ell < 1$ we find that $V(k, p, q) \sim -\ln(q\ell)$ and is essentially independent of k, p . For $|k - p|\ell > 1$ and $q|k - p|\ell^2 < 1$, it is found that $V(k, p, q) \sim -\ln(q|k - p|\ell^2)$. Finally, the matrix element is negligibly small for $q|k - p|\ell^2 > 1$.

For smoother edges this Fermi velocity becomes more and more negative and eventually the system will become unstable to edge reconstructions,^{24–26} signaling a phase transition to a state with a different and more complicated low-energy effective Hamiltonian. However, this instability involves ‘ultraviolet’ physics which is beyond the scope of the present study.

We see from the expression for V_q^{inter} that the inter-edge interaction is important only if $qW < 1$, because the modified Bessel function $K_0(x)$ decays rapidly for $x > 1$. Physically, the Coulomb potential due to a 1D density wave is weak when viewed from a point removed from the 1D system by a distance longer than the period of the wave. For small x , $K_0(x) \rightarrow -\ln[\frac{x}{2}]$ so that in the limit $q \ll W^{-1}$, we have $V_q^{\text{intra}} = V_q^{\text{inter}} = V_q^{\text{QW}}$. The contribution to the Hamiltonian of a quantum Hall bar from modes with a wavelength exceeding W is identical to the corresponding contribution to the effective 1D Hamiltonian for the quantum wire.

IV. BOSONIZATION

TL models described by a Hamiltonian displayed in Eq. (12) can be solved by means of bosonization.^{7–9} This is possible because within the restricted Hilbert space of low-energy, small- q excitations around a uniform ground state, the density operators $\varrho_q^{L,R}$ obey simple bosonic commutation relations. If ν denotes the occupation number of single-particle states in the uniform many-particle ground state around which the excitations occur, the commutation relations are

$$[\varrho_q^L, \varrho_{q'}^L] = \nu \frac{qL}{2\pi} \delta_{q+q',0} \quad (13a)$$

$$[\varrho_q^R, \varrho_{q'}^R] = -\nu \frac{qL}{2\pi} \delta_{q+q',0} \quad (13b)$$

$$[\varrho_q^L, \varrho_{q'}^R] = 0 \quad (13c)$$

So far, we have only considered the case of $\nu = 1$, which is the generic case for a quantum wire. Below we identify ν as the Landau level filling factor of the QH bar and comment on the validity of the Luttinger liquid description of QH edges⁵ at $\nu < 1$.

In order to understand the intriguing features which are special to the physics of a 1D ES, it has proven to be useful⁹ to introduce two new bosonic fields $\theta(x)$ and $\phi(x)$, called *phase fields*. In what follows, we assume that N_R and N_L are fixed. It turns out that the Hamiltonian (12) can then be rewritten (uniquely up to a constant) as a quadratic Hamiltonian in these phase fields. Here, we have an additional motivation for following this procedure; the generalization of the TL picture to fractional filling factors ν is straightforward once the phase fields are introduced. The theory can be formulated in the phase field formalism for an arbitrary filling factor, and the value of ν enters the theory only when calculating physical observables like densities and currents. Before

going into algebraic details, we comment on the justification of the TL model for fractional QH edges. (For a related discussion see Ref. 27.) The explicit derivation for a quantum Hall bar outlined in the previous section does not generalize to the $\nu < 1$ case. However, using arguments based on the analytical structure of many-body wave functions that describe the 2D ES in the fractional QH regime, it can be shown that for abrupt edges the one-to-one correspondence between the low-lying excitations in this system and the excitations of a 1D boson system holds^{4,1} for $\nu = 1/m$ where m is an odd integer. The form of the theory is essentially fixed¹ by this bosonization property and the requirement that the theory recover the fractional quantum Hall effect under appropriate circumstances. Therefore we believe that, for abrupt edges, the low-energy Hamiltonian for a QH bar can be written in the form of Eq. (12) and that the commutation relations Eqs. (13) are valid for the case of $\nu < 1$ also. An exception occurs for large m when the ground state of the 2D ES is expected²⁸ to be a Wigner crystal.

The relation of the phase fields to the densities of left going and right going fermions is given in reciprocal space

$$\theta_q = \sqrt{\frac{\pi}{\nu}} \frac{i}{q} [\varrho_q^R + \varrho_q^L] \quad (14a)$$

$$\phi_q = \sqrt{\frac{\pi}{\nu}} \frac{i}{q} [\varrho_q^R - \varrho_q^L] \quad (14b)$$

We use reciprocal space language for the following discussion because it is convenient for dealing with anomalies caused by the long-range of the electron-electron interaction. The Hamiltonian (12) is quadratic in the phase fields:

$$H = \frac{1}{2L} \sum_q |q| E_q \left\{ \frac{1}{g_q} |\theta_q|^2 + g_q |\phi_q|^2 \right\}. \quad (15)$$

Here E_q is the energy of the low-lying bosonic excitations of the system, generally referred to as plasmons in the quantum wire case and as edge magnetoplasmons in a QH bar. The dispersion relation E_q for the plasmon excitations reads

$$E_q = |q| \left[\hbar v_F + \frac{\nu}{2\pi} V_q^{\text{intra}} \right] \sqrt{(1 + \xi_q)(1 - \xi_q)} \quad (16)$$

and the interaction parameter g_q is defined as

$$g_q = \sqrt{\frac{1 - \xi_q}{1 + \xi_q}}. \quad (17)$$

The parameter ξ_q measures the relative strengths of inter- and intra-edge contributions to the plasmon energy, and its formal expression is

$$\xi_q := \frac{V_q^{\text{inter}}}{V_q^{\text{intra}} + 2\pi\hbar v_F/\nu}. \quad (18)$$

Obviously, $\xi_q = 0$ in the absence of inter-edge interaction. For larger v_F , *i.e.* sharper confining potential, ξ_q is smaller, and we expect corrections due to V_q^{inter} to be less important. Expressions (16) and (18) reflect the interchangeability of one-body and two-body contributions to the plasmon dispersion and V_q^{intra} . Note that in samples with aspect ratios close to unity the value of g_q is close to 1 even at the smallest physically-relevant values of $q \sim L^{-1}$. Using these results we can now compare the physical properties of excitations in quantum wire and QH bar systems.

A. Plasmon Dispersion

In order to do detailed calculations, we must specify the confining potential of the QH bar. In what follows, we adopt the neutralizing background model which produces sharp confinement and diminishes corrections due to the inter-edge interaction as explained above. To calculate the Fermi velocity resulting from a uniform neutralizing background, we can use Eq. (11) apart from a sign change since the Hartree energy of the Fermi sea is simply the electrostatic potential due to the electron charge density in the ground state. With the fractional filling factor incorporated properly, we find that

$$v_F = \nu \frac{e^2}{\hbar \epsilon \pi} \ln \left[\sqrt{2\gamma} \frac{W}{\ell} \right]. \quad (19)$$

For a macroscopic QH sample, W/ℓ is rather large (hence v_F is big), and $W \sim L$. Therefore, the bare Fermi velocity in this system is larger than the renormalization terms arising from interaction effects (V_q^{intra} and V_q^{inter}). It is interesting to compare the $W \sim L$ limit with the case of a perfectly circular quantum dot.^{25,29,30} In that case it follows purely from symmetry arguments that in the long-wavelength limit the plasmon energy is determined completely by the external potential term in the Hamiltonian. We expect this to be approximately true for all samples with aspect ratios close to one. The plasmon dispersion in this limit is

TABLE I. Contributions to the plasmon dispersion in quantum wire and quantum-Hall (QH) bar systems. This Table is based on the common separation of energies in electronic systems into kinetic, Hartree, external potential, and exchange-correlation contributions. Table entries indicate whether the energy mentioned in the left column gives a positive (+), negative (−), or zero (0) contribution to the energy of long wavelength plasmons.

	quantum wire	QH bar
kinetic energy	+	0
external confining potential	0	+
Hartree energy	0	−
exchange/correlation energy	+	+

$$E_q = -\nu \frac{e^2}{\epsilon \pi} |q| \ln \left[\sqrt{\gamma/8} |q| \ell \right]. \quad (20)$$

Expressions of the form of Eq. (20) for the edge magnetoplasmon dispersion have been successfully applied to interpret experimental data^{31–34,36–40} and were originally derived classically^{41,42}. That Eq. (20) is the correct result for experimentally-realistic QH samples is one of the main points of our discussion here. This result should be contrasted with the plasmon dispersion relation at long wavelengths in a quantum wire where (see also Ref. 16) it is found¹⁹ that $E_q \sim |q| \sqrt{|\ln[|q|]|}$. More generally the underlying microscopic terms in the Hamiltonian differ qualitatively in their influence on the magnetoplasmon dispersion in the two cases as summarized in Table I which is based on the common separation of energies into kinetic, Hartree, external potential, and exchange-correlation contributions.

B. Correlation Functions

The phase field formalism facilitates the straightforward calculation of electronic correlation functions. A hallmark of the bosonization approach in the study of 1D systems^{7–9} is the possibility to express the electron field operator ψ in terms of the phase fields. Electron Green's functions can then be written in terms of Green's functions of the phase fields, which are readily calculated because the Hamiltonian (15) is quadratic.

In truly 1D systems, the electron field operator depends on *one* spatial coordinate (x) only. Incorporating the 2D aspect of a quasi-1D ES and, in particular, a QH bar, we have to consider its dependence on the lateral coordinate (y) as well:

$$\psi_{L,R}(x, y) = \Phi_{L,R}(x, y) \exp \left[\pm i \sqrt{\frac{\pi}{\nu}} \theta(x) + i \sqrt{\frac{\pi}{\nu}} \phi(x) \right] \quad (21)$$

where $\Phi_{L,R}^{\text{QW}}(x, y) := \psi_{0,\mp k_F}^{\text{QW}}(x, y)$ for the quantum wire and $\Phi_{L,R}^{\text{HB}}(x, y) := \psi_{0,\mp k_F}^{\text{HB}}(x, y)$ for the QH bar. The operator for the total density of electrons at some position along a quantum Hall bar can be obtained by integrating over the transverse (y) coordinate:

$$\varrho(x) = \int dy [\psi_L(x, y) + \psi_R(x, y)]^\dagger [\psi_L(x, y) + \psi_R(x, y)] \quad (22)$$

In terms of the phase fields we find that

$$\varrho(x) = \sqrt{\frac{\nu}{\pi}} \partial_x \theta(x) + \hat{O}_{\text{CDW}}(x) \quad (23a)$$

where \hat{O}_{CDW} represents the portion of the charge density which oscillates with period π/k_F . The slow decay

of correlations associated with this part of the charge density¹⁵ is the basis of the quasi-crystalline character of the electrons in a quantum wire. The spatial separation of oppositely directed electrons in quantum Hall bars is not important in the first term of Eq. (23a) because the y -dependent part of $\Phi_{L,R}(x, y)$ is normalized. However in the $2k_F$ term, the overlap of $\chi_0(y)$'s at $\pm k_F$ enters and the spatial separation changes the result. We find that

$$\hat{O}_{\text{CDW}}(x) = \frac{1}{\pi\ell} \exp \left[\left(-\frac{W}{2\ell} \right)^2 \right] \cos \left[2k_F x + 2\sqrt{\frac{\pi}{\nu}} \theta(x) \right]. \quad (23b)$$

The quantum wire case can be recovered by setting $W = 0$. In the Hall bar case \hat{O}_{CDW} acquires the prefactor $\exp[-(W/\ell)^2]$ which, for realistic sample dimensions ($W/\ell \sim 10 \dots 100$), is extremely small.

Using the bosonization technique, we find for the CDW correlations

$$\begin{aligned} \langle \hat{O}_{\text{CDW}}(x) \hat{O}_{\text{CDW}}(0) \rangle &= \frac{1}{2\pi^2 \ell^2} \exp \left[- (W/\ell)^2 \right] \cos(2k_F x) \\ &\times \exp \left\{ -\frac{2\pi}{\nu} \langle [\theta(x) - \theta(0)]^2 \rangle \right\}. \end{aligned} \quad (24)$$

The phase field correlation function is determined by the interaction parameter g_q which reflects the non-Fermi-liquid properties of the system⁷⁻⁹ resulting from inter-edge interaction. A standard calculation¹⁵ gives the following result

$$\langle [\theta(x) - \theta(0)]^2 \rangle = \frac{2}{L} \sum_{q>0} g_q \frac{1 - \cos(qx)}{q}. \quad (25)$$

For the case of the Coulomb interaction we find¹⁵ (for $x \geq W$) that

$$\begin{aligned} \langle \hat{O}_{\text{CDW}}(x) \hat{O}_{\text{CDW}}(0) \rangle &= \frac{1}{2\pi^2 \ell^2} \exp \left[- (W/\ell)^2 \right] \cos(2k_F x) \\ &\times \exp \left[-\frac{2}{\nu} \sqrt{|\ln[W/\ell] \ln[x^2/(W\ell)]|} \right]. \end{aligned} \quad (26)$$

The very weak dependence on x at $x \gg W$ is associated with the vanishing of g_q for $qW \ll 1$. The factor $\exp \left[-\frac{2}{\nu} \sqrt{|\ln[W/\ell] \ln[x^2/(W\ell)]|} \right]$ on the r.h.s. of Eq. (26) is plotted as a function of x for two different values of W in Fig. 3. For comparison, the power-law expected when inter-edge interactions are absent

$$\langle \hat{O}_{\text{CDW}}(x) \hat{O}_{\text{CDW}}(0) \rangle \sim \left(\frac{x}{\ell} \right)^{-2/\nu} \text{ if } V_q^{\text{inter}} \equiv 0 \quad (27)$$

is also plotted. The correlations shown in Eq. (26) fall off more slowly than they would if inter-edge interactions were neglected. However, for large W/ℓ , which is the case applicable to QH samples, the relative difference between Eq. (26) and the power-law limit [Eq. (27)] remains small even when x is several times larger than W , see Fig. 3.

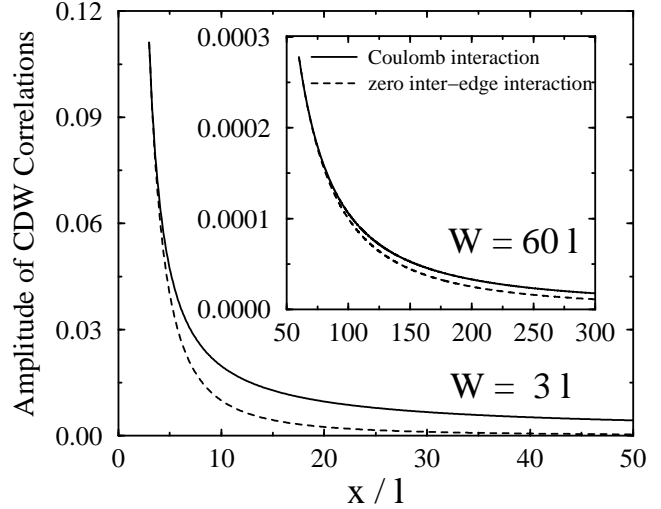


FIG. 3. CDW-correlations at the edge of a QH bar. Plotted as the solid line is the x -dependent exponential on the r.h.s. of Eq. (26) at fixed W/ℓ for filling factor $\nu = 1$. The result $(x/\ell)^{-2/\nu}$ (which one would obtain if inter-edge interaction was not present) is shown as the dotted line. For large W , the difference between the two curves is small for x less than several times W . In samples with large aspect ratios, the correlation functions have a large relative difference for $x \gg W$ but both are already quite small in magnitude. The quasi-solid correlations in quantum wires are therefore unlikely to be of physical importance in typical Hall bar samples.

For Hall bar samples with aspect ratios L/W of order less than ~ 10 , even the minimum value of g_q (for $q = 2\pi/L$) is close to unity. Therefore, there is no regime where quasi-solid correlations occur.

V. SUMMARY

In conclusion, we have calculated microscopically the dispersion relation for edge magnetoplasmons in a QH bar, emphasizing distinctions between these excitations and the plasmon excitations of a quantum wire. We have carefully examined the influence of different terms in the total Hamiltonian on plasmon excitations and obtain quite different results in Hall bar and quantum wire cases. Whereas the plasmon energy in the quantum wire case has contributions only from kinetic energy gain and exchange energy loss in the underlying electron system, the energy of edge magnetoplasmons in a QH bar has additional contributions arising from electrostatic (Hartree) and external potential terms but no contribution due to kinetic energy gain. Despite these differences, the low-energy effective Hamiltonian for both systems is identical for $qW \ll 1$.

Typical sample geometries of QH bars have an aspect ratio close to unity. Therefore, in this case, $qW \geq 1$ even

for the smallest possible q . In this limit, inter-edge interaction is negligibly small. As a result we find that for typical sample geometries, the classical magnetoplasmon dispersion relation, Eq. (20), which differs from the plasmon dispersion relation for a quantum wire, is accurate. Important corrections to the plasmon dispersion due to the interaction between left and right moving parts of the electron density occur only for long narrow Hall bar samples. We also find that typical QH samples are not in the regime where the quasi-solid behavior expected for charge density correlations in a quantum wire is important. Furthermore, the spatial separation of left movers and right movers in a QH bar leads to a suppression of the CDW-fluctuations which is a Gaussian function of the width W of the Hall bar.

ACKNOWLEDGMENTS

The authors acknowledge many helpful discussions with S. M. Girvin, J. J. Palacios, and R. Haussmann. This work was funded in part by NSF grant DMR-9416906. U.Z. thanks Studienstiftung des deutschen Volkes (Bonn, Germany) for financial support.

-
- ¹ See e.g. A. H. MacDonald, Brazilian J. Phys. **26**, 43 (1996).
² In macroscopic samples the charge density profile near the edge of the system is determined primarily by electrostatic considerations. The charge density profile near the edge in many experimental systems varies slowly on a microscopic length scale. See for example D. B. Chklovskii, B. I. Shklovskii, and L. I. Glazman, Phys. Rev. B **46**, 4026 (1992). Microscopic models of the ‘compressible’ strip or strips which occur at smooth edges will generically be more complicated than the single-boson models considered here, see recent work by J. H. Han and D. J. Thouless (cond-mat/9607166).
³ B. I. Halperin, Phys. Rev. B **25**, 2185 (1982).
⁴ A. H. MacDonald, Phys. Rev. Lett. **64**, 220 (1990).
⁵ X. G. Wen, Phys. Rev. B **41**, 12838 (1990).
⁶ X. G. Wen, Int. J. Mod. Phys. B **6**, 1711 (1992).
⁷ V. J. Emery, in *Highly Conducting One-Dimensional Solids*, edited by J. T. Devreese *et al.* (Plenum Press, New York, 1979), pp. 247–303.
⁸ J. Sólyom, Adv. Phys. **28**, 201 (1979).
⁹ F. D. M. Haldane, J. Phys. C **14**, 2585 (1981).
¹⁰ Advanced lithographic techniques are leading to increased experimental and theoretical interest in semiconductor quantum wire systems. For recent reviews, see *Quantum Transport in Ultrasmall Devices*, NATO ASI Series Vol. B342, edited by D. K. Ferry *et al.* (Plenum Press, New York, 1995).
¹¹ Y. Oreg and A. M. Finkelstein, Phys. Rev. Lett. **74**, 3668 (1995).
¹² K. Moon and S. M. Girvin, Phys. Rev. B **54**, 4448 (1996).
¹³ M. Fabrizio, A. O. Gogolin, and S. Scheidl, Phys. Rev. Lett. **72**, 2235 (1994).
¹⁴ H. Maurey and T. Giamarchi, Phys. Rev. B **51**, 10833 (1995).
¹⁵ H. J. Schulz, Phys. Rev. Lett. **71**, 1864 (1993).
¹⁶ For long narrow quantum Hall bars the analogy with quantum wires is closer. See M. Franco and L. Brey, Phys. Rev. Lett. **77**, 1358 (1996).
¹⁷ In this paper we assume that the field is strong enough that $m^*\omega_c^2$ always exceeds the curvature of the confining potential.
¹⁸ M. Büttiker, Phys. Rev. B **38**, 9375 (1988).
¹⁹ S. Das Sarma and Wu-yan Lai, Phys. Rev. B **32**, 1401 (1985); Q. P. Li, S. Das Sarma, and R. Joynt, Phys. Rev. B **45**, 13713 (1992).
²⁰ A. Gold and A. Ghazali, Phys. Rev. B **41**, 7626 (1990).
²¹ J. M. Kinaret and P. A. Lee, Phys. Rev. B **42**, 11768 (1990).
²² X. G. Wen, Phys. Rev. B **44**, 5708 (1991).
²³ J. Dempsey, B. Y. Gelfand, and B. I. Halperin, Phys. Rev. Lett. **70**, 3639 (1993).
²⁴ C. de C. Chamon and X. G. Wen, Phys. Rev. B **49**, 8227 (1994).
²⁵ A. H. MacDonald, S. R. Yang, and M. D. Johnson, Aust. J. Phys. **46**, 345
²⁶ Y. Meir, Phys. Rev. Lett. **72**, 2624 (1994); L. Brey, Phys. Rev. B **50**, 11861 (1994); O. Klein *et al.*, Phys. Rev. Lett. **74**, 785 (1995).
²⁷ M. Stone and M. P. A. Fisher, Int. J. Mod. Phys. B **8**, 2539 (1994).
²⁸ See e.g. X. Zhu and S. G. Louie, Phys. Rev. Lett. **70**, 335 (1993); R. Price, P. M. Platzman, and S. He, Phys. Rev. Lett. **70**, 339 (1993); and references cited therein.
²⁹ S. Giovanazzi, L. Pitaevskii, and S. Stringari, Phys. Rev. Lett. **72**, 3230 (1994).
³⁰ A. I. Andreev, Ya. M. Blanter, and Yu. E. Lozovik, Int. J. Mod. Phys. B **9**, 1843 (1995).
³¹ S. J. Allen, H. L. Störmer, and J. C. M. Hwang, Phys. Rev. B **28**, 4875 (1983).
³² V. I. Tal’yanskii, JETP Lett. **43**, 127 (1986).
³³ T. Demel, D. Heitmann, P. Grambow, and K. Ploog, Phys. Rev. Lett. **64**, 788 (1990).
³⁴ M. Wassermeier *et al.*, Phys. Rev. B **41**, 10287 (1990).
³⁵ I. Grodnensky, D. Heitmann, and K. von Klitzing, Phys. Rev. Lett. **67**, 1091 (1991).
³⁶ R. C. Ashoori *et al.*, Phys. Rev. B **45**, 3894 (1992).
³⁷ N. B. Zhitenev, R. J. Haug, K. v. Klitzing, and K. Eberl, Phys. Rev. Lett. **71**, 2292 (1993).
³⁸ D. B. Mast, A. J. Dahm, and A. L. Fetter, Phys. Rev. Lett. **54**, 1706 (1985).
³⁹ D. C. Glatli *et al.*, Phys. Rev. Lett. **54**, 1710 (1985).
⁴⁰ P. J. M. Peters *et al.*, Phys. Rev. Lett. **67**, 2199 (1991).
⁴¹ V. A. Volkov and S. A. Mikhailov, Zh. Eksp. Teor. Fiz. **94**, 217 (1988) [Sov. Phys. JETP **67**, 1639 (1988)].
⁴² Ya. M. Blanter and Yu. E. Lozovik, Physica B **182**, 254 (1992).